January 1, 2009

Persistent West Nile virus associated with a neurological sequela in hamsters identified by motor unit number estimation

V Siddharthan
H Wang
N E Motter
J O Hall
R D Skinner, et al.

Journal of Virology

Persistent West Nile Virus Associated with a Neurological Sequela in Hamsters Identified by Motor Unit Number Estimation

Venkatraman Siddharthan, Hong Wang, Neil E. Motter, Jeffery O. Hall, Robert D. Skinner, Ramona T. Skirpstunas and John D. Morrey

Updated information and services can be found at:
http://jvi.asm.org/content/83/9/4251

These include:

REFERENCES
This article cites 46 articles, 21 of which can be accessed free at: http://jvi.asm.org/content/83/9/4251#ref-list-1

CONTENT ALERTS
Receive: RSS Feeds, eTOCs, free email alerts (when new articles cite this article), more»

Vol. 83, No. 9

Persistent West Nile Virus Associated with a Neurological Sequela in Hamsters Identified by Motor Unit Number Estimation[▽]

Venkatraman Siddharthan,[1] Hong Wang,[1] Neil E. Motter,[1] Jeffery O. Hall,[1] Robert D. Skinner,[2]
Ramona T. Skirpstunas,[1] and John D. Morrey[1]*

*Institute for Antiviral Research, Department of Animal, Dairy, and Veterinary Sciences, Utah State University, Logan, Utah 84322,[1]
and Center for Translational Neuroscience and Department of Neurobiology and Developmental Sciences, University of
Arkansas for Medical Sciences, Little Rock, Arkansas 72205[2]*

To investigate the hypothesis that neurological sequelae are associated with persistent West Nile virus (WNV) and neuropathology, we developed an electrophysiological motor unit number estimation (MUNE) assay to measure the health of motor neurons temporally in hamsters. The MUNE assay was successful in identifying chronic neuropathology in the spinal cords of infected hamsters. MUNE was suppressed at days 9 to 92 in hamsters injected subcutaneously with WNV, thereby establishing that a long-term neurological sequela does occur in the hamster model. MUNE suppression at day 10 correlated with the loss of neuronal function as indicated by reduced choline acetyltransferase staining ($R^2 = 0.91$). Between days 10 and 26, some α-motor neurons had died, but further neuronal death was not detected beyond day 26. MUNE correlated with disease phenotype, because the lowest MUNE values were detected in paralyzed limbs. Persistent WNV RNA and foci of WNV envelope-positive cells were identified in the central nervous systems of all hamsters tested from 28 to 86 days. WNV-positive staining colocalized with the neuropathology, which suggested that persistent WNV or its products contributed to neuropathogenesis. These results established that persistent WNV product or its proteins cause dysfunction, that WNV is associated with chronic neuropathological lesions, and that this neurological sequela is effectively detected by MUNE. Inasmuch as WNV-infected humans can also experience a poliomyelitis-like disease where motor neurons are damaged, MUNE may also be a sensitive clinical or therapeutic marker for those patients.

An understanding of the different phases of West Nile virus (WNV) disease is important to understand the natural history and the prevention and control of the disease. The initial infection leading to the viremic phase elicits innate (31, 39) and acquired (e.g., WNV-specific cytotoxic T lymphocytes) (41) immune responses. The West Nile fever syndrome may be associated with this phase of infection, which involves fever, headache, malaise, fatigue, and nausea. The virus can infect the central nervous system (CNS) to cause acute neurological clinical syndromes, such as meningitis, encephalitis, and paralysis (13, 34). The innate and acquired immune responses participate to prevent, reduce, or eliminate viral load in the CNS, but they may also contribute to neuroimmunopathology (11). The resulting neurological damage can persist as long-term neurological sequelae, which are widespread among survivors. The pathogenesis and cause of neurological sequelae have not been established, nor is the role that the virus plays in long-term disease known (13, 34).

Some evidence suggests that WNV can establish a persistent infection, which may adversely affect neuronal tissues. WNV was isolated from rhesus monkey brains up to 5½ months after intracerebral inoculations; and the monkeys from which these viruses were isolated possessed subacute inflammatory neurodegeneration of the CNS (27). This property of persistence is shared with some other flaviviruses, (i.e., tick-borne encephalitis virus in primates) (28), Japanese encephalitis virus in pregnant mice (20), Modoc virus in hamsters (8), and St. Louis encephalitis virus in hamsters (40). These preliminary data provided impetus for the hypothesis that neurological sequelae are associated with persistent WNV infection and neuropathology.

Our data (32) and the research of others (38) have established that WNV infects neurons, among which are large α-motor neurons in the spinal cord, to cause cellular damage or death involving apoptotic signaling or necrosis (4). The loss of motor neurons is detected in other neurodegenerative diseases, such as amyotrophic lateral sclerosis (ALS) (30, 36) and poliomyelitis (25), by using electrophysiological motor unit number estimation (MUNE) (5), in which a motor unit consists of an α-motor neuron and all the muscle fibers it innervates. A presumptive use of MUNE in the human WNV infection was identified in an uncontrolled clinical study (2) in which MUNE appeared to be a marker for degrees of weakness and recovery in patients with neurological sequelae.

In this study, we establish that WNV can persistently infect neurons to cause dysfunction, that WNV is associated with chronic neuropathological lesions in the spinal cord, and that this neurological sequela as detected by MUNE is nearly a universal event in WNV-infected hamsters.

MATERIALS AND METHODS

Animals and viruses. Adult female Syrian golden hamsters greater than 7 weeks of age were used (Charles River Laboratories). Animals were randomized to treatment groups. This study was conducted in accordance with the approval of the Institutional Animal Care and Use Committee of Utah State University.

One New York isolate (NY WNV) (18, 19) from crow brain (7) and one from an owl (385-99, TVP 7767; Robert Tesh, University of Texas Medical Branch Arbovirus Reference Collection) (46) were used. Two isolates of the emerging dominant genotype (WN02) were used: one isolate from bird 114 (TX-114; Robert Tesh) and one isolate from bird 113 (TX-113) (Biodefense and Emerging Infectious Research Resources Repository, Manassas, VA). Four different WNV isolates were used to eliminate concerns about the results being WNV isolate specific and because the different isolates had characteristics more suitable for specific studies. The WN02 TX-113 strain was particularly useful for the study of long-term neurological sequelae because of the higher survival rate compared to the NY WNV strains and the slightly higher pathogenicity compared to TX-114. The NY isolate 385-99 was used for the paralysis studies, since WN02 isolates did not readily cause paralysis. The NY 385-99 and WN02 TX-113 strains were used for histopathological studies in order to have a representative isolate of each WNV strain. Different challenge doses of the viruses were required due to the variable pathogenesis of the viral stocks in hamsters. Animals were injected subcutaneously (s.c.) with 5.3×10^7 PFU of NY WNV (crow brain isolate), 1.2×10^4 PFU of NY WNV 385-99, 1.2×10^4 PFU of TX-113, and 1.3×10^6 PFU of TX-114. The viruses were propagated in MA-104 cells and diluted in minimal essential medium (MEM) immediately prior to s.c. injection in the groin area with a volume of 100 μl. The use of Punta Toro virus in hamsters (12) and the use of yellow fever virus in hamsters (14) are described elsewhere.

Electrophysiological methods. An incremental step stimulation protocol in mice (36, 37) was applied to hamsters to measure the MUNE. Hamsters were anesthetized and maintained throughout the whole procedure with isoflurane (2% in ~1 liter of O_2 per min). The animals were placed on a platform to support the head and torso to allow their limbs to hang freely. The hind limb and dorsal thigh were sheared and scrubbed with iodine solution and ethanol. The stimulus acupuncture needles (Tai Chi Brand 40 gauge; Lhasa OMS, Inc., Weymouth, MA) were inserted close to the rostral sciatic nerve, and the ground needle was placed s.c. at the dorsal thigh. The motor responses were recorded at the lower hind limb at the gastrocnemius muscle using the pre-gelled self-adhesive disposable disk electrodes (Viasys Healthcare, Madison, WI). The disks were trimmed to 0.4 cm and 0.7 to 1.0 cm to conveniently wrap circumferentially around the distal hind limb. Animals were grounded using a wire with an alligator clip attached to a nonirritating and nonadhesive conductive gel applied onto their tails, and the other end of the wire was attached to the grounded table.

The stimulus was a monophasic square wave at a 0.1-ms duration delivered by an Isostim stimulator/isolator A320 (World Precision Instruments, Sarasota, FL), which was connected with the stimulus needle via a resistor (1 kΩ) to convert current flow to a voltage potential. The recording electrodes were connected to shielded wires and to a DAM50 bioamplifier (World Precision Instruments, Sarasota, FL), which was kept inside the copper mesh cage to avoid interference. The LabVIEW 8.2 virtual instrument program (National Instruments Corporation, Austin, TX) interfaced with the computer was used for initiating the stimulation and for recording of the biopotential energy.

One-hundred-fold gain was used to amplify the biopotential energy. To identify the incremental quantum steps from the threshold to the maximal amplitude of the M-wave depolarization and polarization voltages, the voltage was adjusted during 1-Hz stimulations. Stimulus intensity was slowly increased to determine the response threshold. Quantum jumps in the amplitude of the M-wave were recorded after observing three to five similar responses. This process was repeated until no more quantum jumps were observed. The supramaximal M-wave was used as the compound muscle action potential. The average mV of the increment (surface motor unit action potential in mV) was divided into the compound muscle action potential to obtain MUNE (36, 37). For each measurement, 200 to 300 data points were recorded at a sampling rate of 10,000 Hz; thus, the x axis was 0.1 ms per data point. The graphs were constructed with each line as 1/50 of the RGB rainbow, such that the greater number of MUNE increments produces more of the color spectrum beginning with yellow, to orange, to red, and to blue. The y axis is the action potential in mV, but these units are typically not shown in the literature, because the absolute values of action potentials are not important for the interpretation of the data; rather the measurements between the quantum jumps are necessary for interpretation as explained above.

Histology. Paraffinized sections were used for hematoxylin and eosin (H&E) and confocal microscopy for the detection of WNV envelope, neuron-specific enolase (NSE), and terminal deoxynucleotidyl transferase-mediated dUTP-biotin nick end labeling (TUNEL) staining. Cryostat sections were used with peroxidase staining for WNV envelope, choline acetyltransferase (ChAT), and Nissl staining.

To prepare tissues for fluorescence immunohistochemistry (see Fig. 10) and H&E staining (see Fig. 5 and 7), cardiac perfusion with phosphate-buffered saline followed by 200 ml of freshly prepared 4% paraformaldehyde was per-

formed (24). Paraffinized sections were processed using primary monoclonal antibody 7H2 against WNV (BioReliance, Invitrogen Bioservices, Rockville, MD) and Alexa Fluor 568 goat anti-mouse immunoglobulin G (IgG) antibody for WNV detection. Primary polyclonal anti-NSE antibody (Chemicon, Temecula, CA) and Alexa Fluor 488 goat anti-mouse IgG antibody (Molecular Probes, Eugene, OR) were used for NSE detection. Stained slides were visualized using a Nikon Eclipse TE300 microscope (Nikon) attached with Lambda DG4 (Sutter Instrument Company, Novato, CA) and a Bio-Rad MRC 1024 confocal microscope (Bio-Rad, Hercules, CA). A board-certified veterinary pathologist examined the H&E-stained sections under a blinded evaluation protocol.

To detect the WNV envelope antigen (Fig. 5), the cryostat sections were subsequently stained with monoclonal antibody 7H2 for WNV envelope and horse anti-mouse IgG (1:200 BA-1000; Vector Lab) with the avidin-biotin-peroxidase complex detection system (1:100, Vectastain ABC kit; Vector Lab). The chromogen reaction used 0.3% hydrogen peroxide and 3,3′-diaminobenzidine.

ChAT and Nissl staining (see Fig. 3) (6) was performed on 12-μm cryostat sections attached to poly-L-lysine-coated glass slides. Sections were incubated with 0.5% Triton X-100 for 1 h, blocked with normal goat serum for 30 min at room temperature, incubated with rabbit anti-ChAT polyclonal primary antibody (1:2,000, AB5042; Chemicon, Temecula, CA) at 4°C overnight, incubated with biotinylated goat anti-rabbit IgG (1:200, BA-1000; Vector Lab, Burlingame, CA) for 2 h at room temperature, and stained with the avidin-biotin-peroxidase complex kit (1:100, Vectastain ABC kit; Vector Lab) for 30 min. Tissue-bound peroxidase complex was visualized by chromogen reaction with 0.3% hydrogen peroxide and 3,3′-diaminobenzidine (Sigma, St. Louis, MO) containing 0.15 mg/ml nickel-ammonium sulfate for 10 to 15 min. Between each incubation step, the sections were carefully rinsed in several changes of phosphate-buffered saline and water. Sections were dehydrated and mounted with permanent mounting medium (Permount; Fisher Scientific). For the Nissl staining (Fig. 3), cryostat sections were stained with cresyl violet solution (FD Neuro Technologies Consulting and Services, Baltimore, MD) for 5 to 10 min, rinsed briefly in distilled water, soaked in 95% ethanol in 0.1% glacial acetic acid for 1 min, dehydrated in 100% ethanol, cleared with xylene, and mounted with coverslips using mounting medium.

ChAT-stained α-motor neurons were counted in the ventral horns of serial coronal sections (44) from the lumbosacral cord. ChAT-stained α-motor neurons were counted in every other serial section, and the Nissl-stained α-motor neurons were counted in the other alternating sections. For each animal, the average number of positively stained cells per spinal cord section was calculated, wherein 20 to 25 spinal cord sections were counted for both ChAT and Nissl.

WNV RNA. Quantitative reverse transcription-PCR (qRT-PCR) was used to assay the WNV-specific RNA (15, 22). Fresh tissues were homogenized in Trizol RNA purification reagent (Sigma-Aldrich Chemical). Primer pairs and qRT-PCR algorithms for measurement of WNV RNA and mouse glyceraldehyde phosphate dehydrogenase from tissues were described previously (16). A standard curve generated from serial dilutions of a positive sample was used to determine the relative WNV RNA per gram of tissue.

Cocultivation. Two cocultivation methods were employed. One method (29) involved trypsin treatment and cocultivation of viable tissue cells onto Vero cells. The other was involved homogenizing the tissue in a 1:1 ratio (wt/vol) with MEM and freezing the homogenate. A volume of 50 μl of 1:5 diluted homogenate was added to a monolayer of >85% confluent Vero cells in six-well plates. Virus was allowed to absorb for 2 h at 37°C, and then the homogenate was rinsed from the monolayers with MEM–5% fetal bovine serum. The cells were cultivated for 6 days, during which any cytopathic effect was noted. Cell monolayers were frozen and then thawed, and 500 μl was added to Vero cells for a second passage of presumptive virus. Three passages were completed wherein the tissues were identified as infectious virus positive if a cytopathic effect emerged. RT-PCR was used to confirm both the negative and positive cultures.

RESULTS

MUNE. In one of two longitudinal experiments in which MUNE was measured on days 4, 7, and 10 after WN02 subcutaneous injection, the MUNE values at days 4 and 7 were 99.6% and 87.9% of those of the sham-infected animals, respectively (Fig. 1A). However, by day 10, MUNE values were 58.7% of sham controls and were statistically different from MUNE values at day 4 ($P \leq 0.001$). Neurons in the spinal cords of animals were confirmed to be infected with WNV at
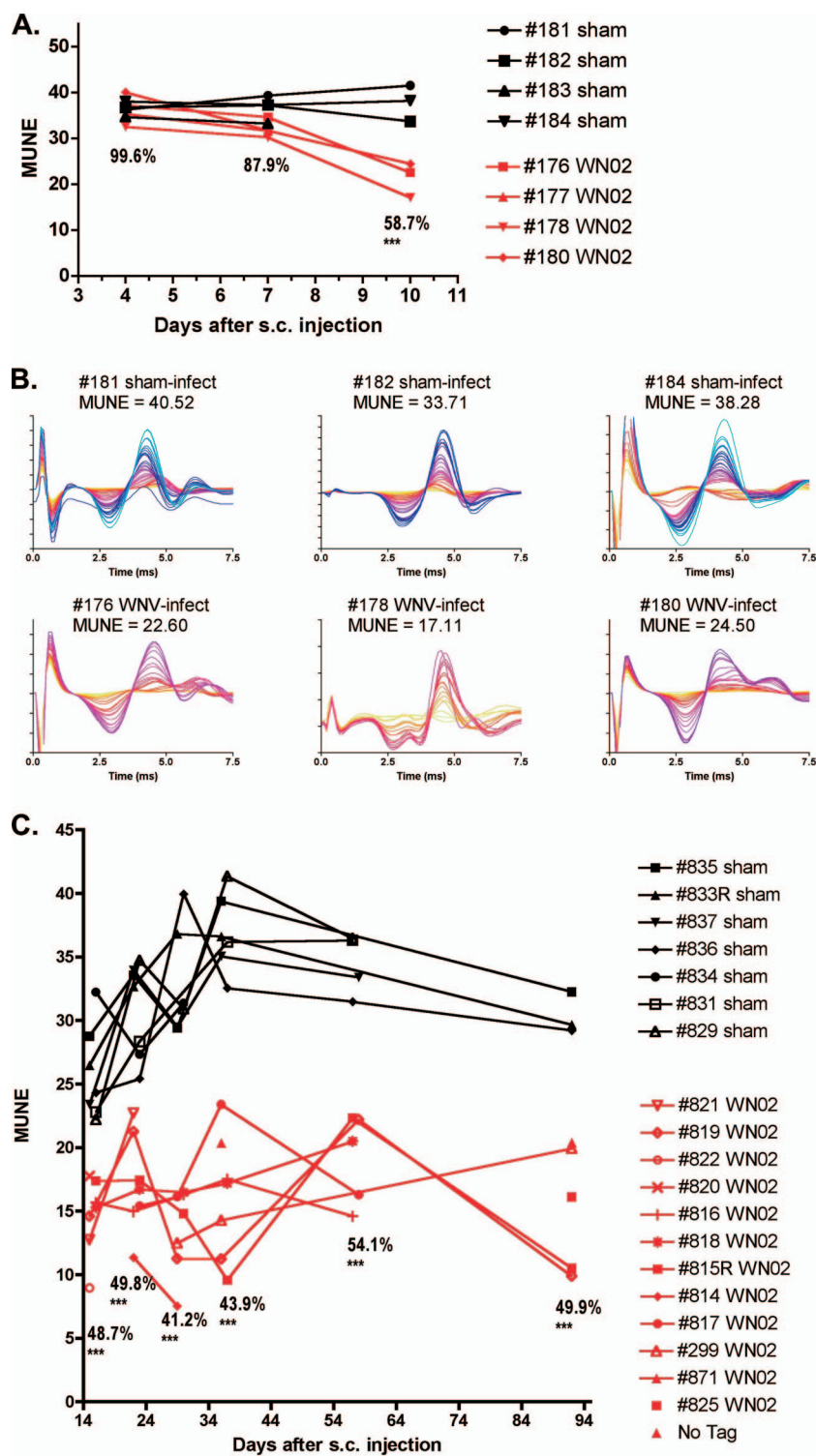
FIG. 1. MUNE of hamsters injected s.c. with WN02 (TX-113) or sham infected. (A) MUNE values from days 4 through 10 showing values of injected animals as a percentage of those of sham-infected controls. Statistical significance was calculated by comparing the percent reduction of MUNE with MUNE at day 4 (∗∗, $P \leq 0.01$ by t test). (B) MUNE tracings at day 10. The graphs were constructed such that the greater number of MUNE increments produces more of the color spectrum beginning with yellow, to orange, to red, and to blue. (C) MUNE of hamsters 15 to 92 days after s.c. injection with WN02 (TX-113) or sham-controls. ∗∗∗, $P \leq 0.001$ by analysis of variance and Newman-Keuls multiple comparison test compared with day 4.
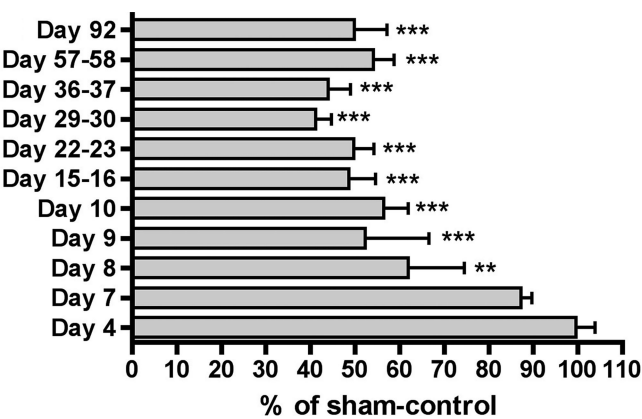
FIG. 2. MUNE values from days 4 to 92 in infected hamsters as a percentage of those of sham-infected controls. Animals were injected s.c. with the WN02 TX-113 isolate and monitored for MUNE. **, $P < 0.01$, and ***, $P < 0.001$, by analysis of variance and Newman-Keuls multiple comparison test compared with day 4.

day 10 (data not shown). The individual MUNE tracings of the animals on day 10 are shown (Fig. 1B). To determine if MUNE returned to normal, remained the same, or decreased further over a long period of time, a second longitudinal experiment

was done in which MUNE was measured between days 15 and 92 (Fig. 1C). MUNE values were suppressed at every time point ($P \leq 0.001$).

Subsequent to the two experiments described above, MUNE was measured in additional infected animals at days 7, 8, and 9. The data from all experiments are summarized in Fig. 2 as a percentage of those from sham-infected controls. MUNE was significantly suppressed at day 8 ($P \leq 0.01$) and rapidly reached a maximum suppression soon thereafter ($P \leq 0.001$), with suppression lasting through the end of the experiment at day 92.

Association of MUNE with neurological disease. To verify the specificity of MUNE as a marker for West Nile neurological disease in hamsters, MUNE was measured in hamsters infected with viruses that do not cause neurological disease. MUNE values of diseased hamsters infected with yellow fever, a flavivirus (31.3 ± 2.7; $n = 3$), or with Punta Toro virus, a bunyavirus (34.8 ± 6.5; $n = 3$), were greater than the normal value cutoff of <21.

As additional proof, MUNE values were compared to ChAT (Fig. 3A), a marker in the spinal cord for functional motor neurons, and to α-motor neurons identified by the Nissl stain (Fig. 3B) assayed at day 10 in the ventral horn of the lumbo-
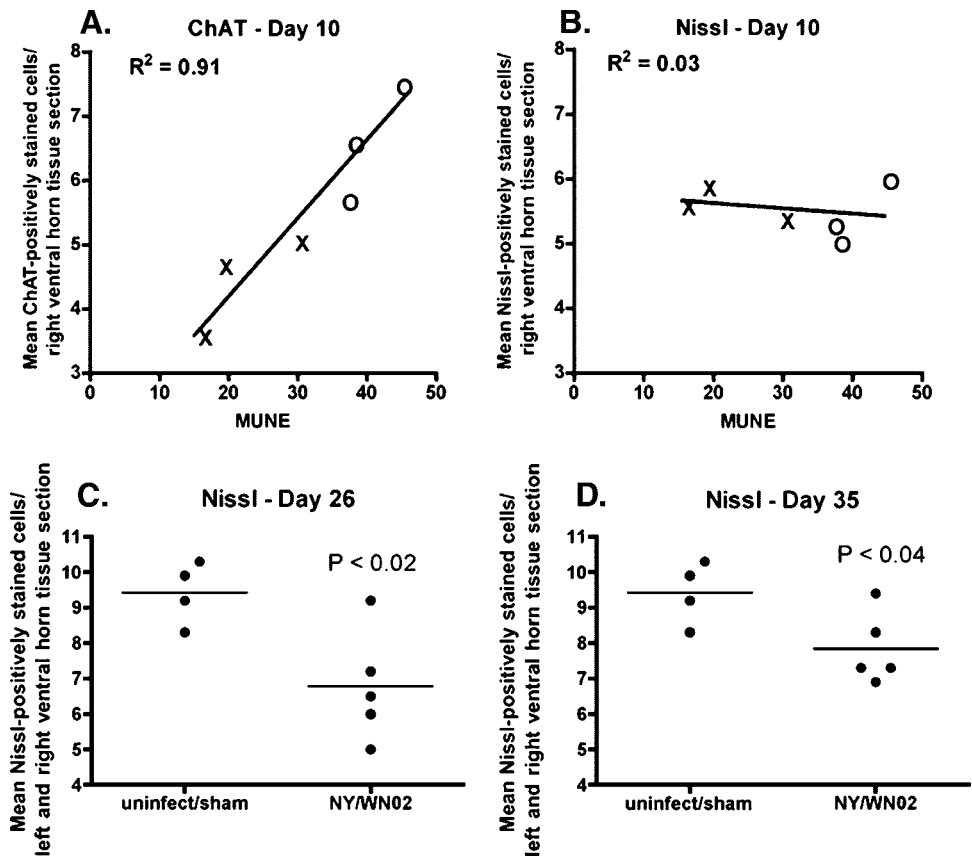

FIG. 3. ChAT and Nissl staining of α-motor neurons in the spinal cord correlated with MUNE. (A and B) ChAT (A) and Nissl (B) staining of α-motor neurons in right ventral horn of the lumbosacral spinal cord of hamsters injected s.c. with WNV (WN02 TX-113 isolate) correlated with MUNE values at 10 dpi. The right horn was counted because the right leg was measured for MUNE. Every other section of the lumbosacral cord was stained. Shown are average counts per section of at least 25 sections that stained and were counted with ChAT or Nissl per animal. (×, infected; ○, sham infected). (C and D) Nissl staining of α-motor neurons in both sides of the ventral horn of the lumbosacral spinal cord of hamsters injected s.c. with WNV (WN02 or NY WNV crow brain isolates) at 26 (C) or 35 (D) days postinjection. uninfect, uninfected.
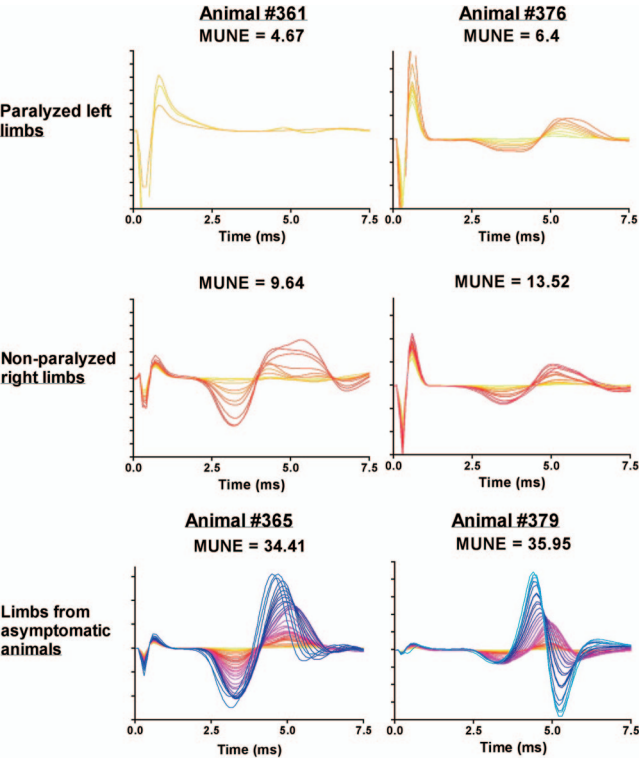
FIG. 4. MUNE tracings from hind limbs of WNV-infected hamsters with paralysis or no paralysis. Hamsters were all injected s.c. with NY WNV (isolate 385-99). Animals #361 and #376 became paralyzed in the left limb on 11 and 12 dpi, respectively, and were assayed on those days for MUNE in both limbs. Limbs from asymptomatic infected animals were assayed on day 11 (#365) and on day 12 (#379).

FIG. 5. WNV envelope staining at 43 days after s.c. injection of NY WNV (crow brain isolate) in a moribund hamster. Scale bar, 20 μm.

of foci are shown (Fig. 5) in the frontal cortex and in the hippocampus. Stained WNV foci like these were occasionally observed in the histological sections of this animal, whereas no staining was observed in most of the brain.

As additional proof of persistent virus, WNV RNA was semiquantified by RT-PCR in homogenized neurological tissues from hamsters infected s.c. with either WN02 (TX-114) or NY WNV (crow brain isolate) at 28, 35, or 89 days post-viral injection (dpi). WNV RNA was identified in all neurological tissues (cerebellum; cerebral cortex; midbrain; and cervical, thoracic, and lumbar spinal cord) and from all infected hamsters (Fig. 6). Spinal cord tissues had overall higher WNV RNA titers than the brain tissues, and the cerebral cortex had the lowest overall titers. The two WN02-infected hamsters at 89 dpi appeared to have the highest titers, and #551 (NY WNV at 28 dpi) appeared to have the lowest titers overall, followed by #560 (NY WNV at 28 dpi) or #562 (WN02 at 35 dpi). No WNV RNA was detected in any tissues of the uninfected animal. To determine if infectious virus could be recovered from these tissues, the frozen homogenized tissues were cocultivated with Vero cells and passed three times. Infectious

sacral cord. Remarkably, MUNE strongly correlated with the number of ChAT-stained neurons of both the infected and sham-infected animals ($R^2 = 0.91$, $P \leq 0.01$ using the Pearson r test), but it did not correlate with Nissl-stained neurons at 10 days post-viral injection ($R^2 = 0.03$). By days 26 and 35, however, the numbers of Nissl-stained neurons from infected animals were statistically reduced by 28% and 18%, respectively, compared to sham-infected and uninfected animals, which indicated that neurons lost function first, after which some dysfunctional motor neurons died between days 10 and 26 but did not continue to die past day 26 (Fig. 3C and D).

To evaluate MUNE as a marker for hind limb paralysis, we measured the MUNE in WNV-infected hamsters with different levels of hind limb paralysis (Fig. 4). The MUNE values of paralyzed limbs from two hamsters were the lowest values observed in these series of studies (4.67 and 6.4), whereas the MUNE values of nonparalyzed limbs from the same animals were higher (9.64 and 13.52). The MUNE values from limbs of infected, but asymptomatic hamsters with no overt disease signs were within normal ranges (34.41 and 35.95).

Persistent WNV. Since MUNE was suppressed long after the acute phase of the disease through day 92, we investigated the possibility that WNV can persist in the CNS of s.c.-injected hamsters. Cryostat sections of the brain from a hamster that appeared moribund at 43 days after s.c. injection of NY WNV (crow brain isolate) was stained for WNV envelope. Examples
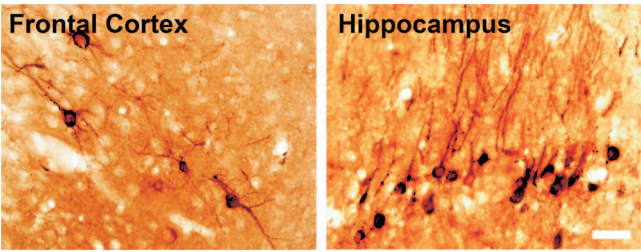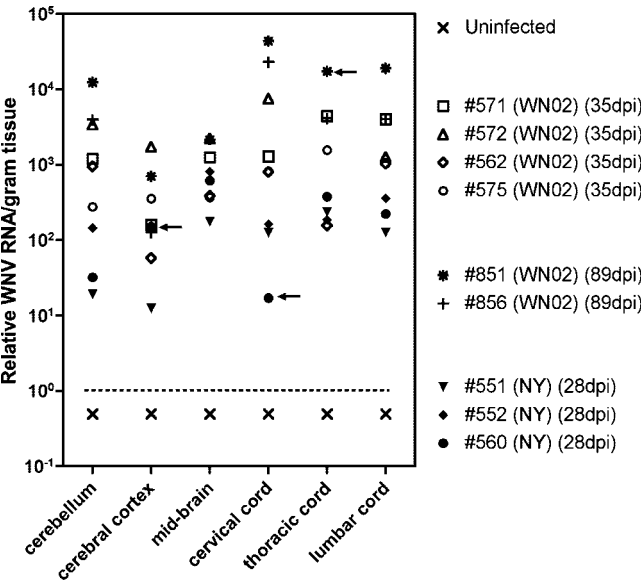

FIG. 6. WNV RNA titers in neurological tissues at 28, 35, or 89 dpi. Hamsters were infected s.c. with either WN02 (TX-114) or NY WNV (crow brain isolate). Arrows indicate samples from which infectious virus was recovered from frozen tissues cocultivated with Vero cells.
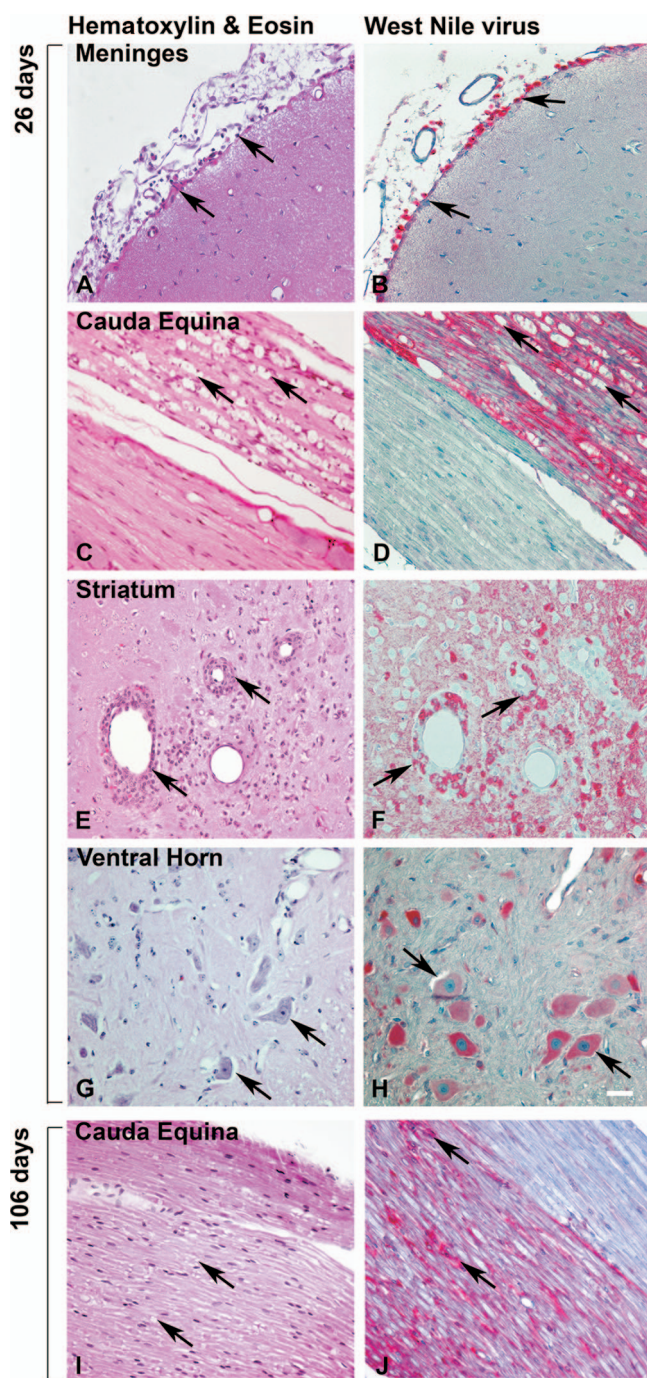
FIG. 7. Representative sequential histological sections from WNV-infected hamsters at 26 or 106 dpi. Hamsters injected s.c. with NY WNV strain 385-99 (A, B, C, and D) and WN02 TX-113 (E, F, G, and H) at day 26 were stained with either H&E (A, C, E, and G) or underwent WNV envelope staining (B, D, F, and H). (I and J) Sections stained at day 106. Arrows show pathology of WNV-stained cells. Scale bar, 20 μm.

detected could be due to the presence of viral RNA or protein in long-lived neuronal cells without the survival of infectious virus. Alternatively, genotypic adaptation may have altered the ability to detect infectious virus in the Vero indicator cells.

Association of viral antigen with neuropathology. To determine if the presence of virus correlated with neuropathology, CNS tissues from three animals at 26 days after s.c. injection of WN02 were stained for WNV envelope antigen and adjacent serially sectioned slides were stained with H&E to identify neuropathology. Representative images are shown in Fig. 7, although the pathologies described occurred in all animals. All areas with cerebral meningitis (Fig. 7A and B), perivascular cuffing, and cellular infiltration were associated with WNV-stained lymphoid-like cells (Fig. 7E and F), whereas areas with no pathology were not stained with WNV. Astrocytic or microglial cells in these sections were not obviously stained for WNV envelope. In the lumbosacral spinal cord, WNV staining was associated with α-motor neurons (Fig. 7G and H). Rare axon bundles in the cauda equina were confluently stained for WNV envelope antigen, whereas the adjacent axon bundles were completely negative for WNV staining. Most notably, those axon bundles positive for WNV staining had extensive axonal swelling (Fig. 7C and D), but no such pathology was present in adjacent axon bundles, which demonstrated strong association of WNV staining with neuropathology. Normal tissues were not associated with WNV-stained cells. As late as day 106, WNV-positive staining also correlated with pathology in the cauda equina (Fig. 7I and J).

Anatomical location of neuropathology. To map the neuropathogenesis in the brain of hamsters, H&E sections were examined qualitatively for neuropathology at 26 dpi from the whole brains of two hamsters injected s.c. with NY WNV, two hamsters injected with WN02 (TX-113), one sham-infected hamster, and one normal hamster (Fig. 8). All four of the surviving infected hamsters when assayed at day 26 possessed neuropathology having some or all of the following lesions: meningitis, gliosis, lymphocyte infiltration, perivascular lymphocyte cuffing, or some neuronal necrosis. More lesions were apparent in the rostral part of the brain. More specifically, lesions were found predominantly in the frontal cortex, striatum, piriform cortex, and entorhinal cortex. Predominant lesions were also identified in the hippocampus and hypothalamus (data not shown). All four hamsters possessed some lesions in the brain stem or cerebellum, but the extent of the lesions was less than in the rostral area of the brain. No pathology, other than rare and very mild meningitis, was apparent in the sham-infected or normal hamsters.

We examined H&E sections of the spinal cord from the same animals in which we examined the brain (Fig. 9). Lesions were observed throughout the spinal cord, but the caudal end of the lumbosacral cord had the most lesions, followed by the cervical cord: i.e., fewer lesions were noted in the thoracic cord. Gliosis and lymphocytic infiltration were the most common lesions, followed by very limited neuronal degeneration in the lumbar cord, perivascular cuffing in the lumbar cord, and a small amount in the cervical cord. Spinal meningitis was not readily observed. Although the NY strain of WNV may have caused more pronounced lesions than the WN02 strain, the pattern of distribution throughout the spinal cord did not seem to be strain specific. Most of the lesions in the lumbosacral

virus was recovered in only 3 of 52 tissues (5.7%) as determined by cytopathic effect and RT-PCR (Fig. 6), but we cannot rule out that these three positive cultures were not due to WNV contamination. The lack of recovery of infectious virus from tissues in which viral RNA and envelop antigen were
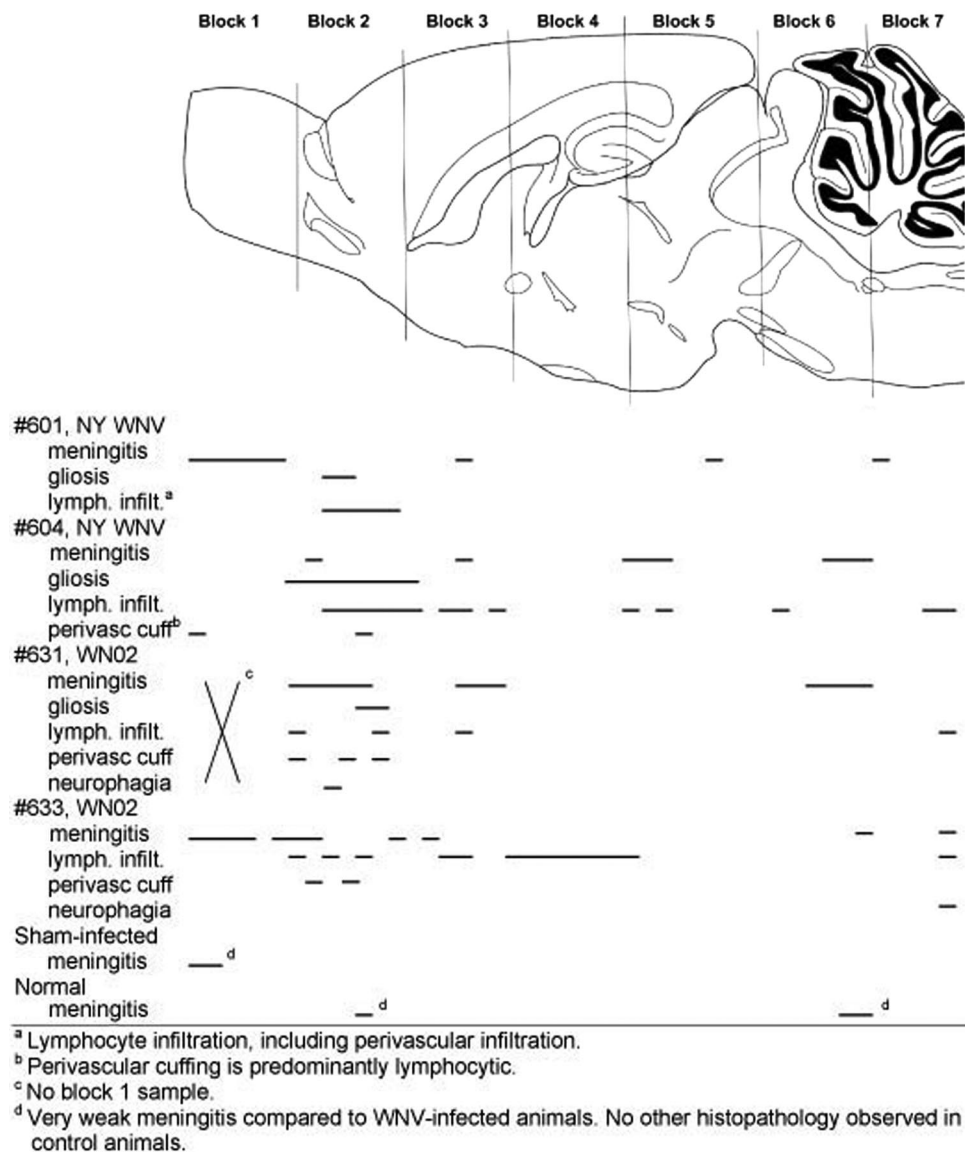
FIG. 8. Mapping neuropathology in the brain of hamsters injected s.c. with WNV. Hamsters were injected s.c. with strain WN02 TX-113 or NY WNV (385 to 99). At 26 days after challenge, the whole brain was cut into coronal sections of five 5-μm sections followed by a 50-μm gap and repeated with the next five sections followed by a gap. The first slide in each of five sections was processed for H&E staining. Horizontal lines were used to map the location of the lesions within the brain.

cord were located in the ventral horn of the gray matter, although some lymphocytic infiltration and gliosis were observed in the dorsal and lateral gray matter of the cervical and thoracic cords. Lymphocytic infiltration, gliosis, and myelin sheath swelling were observed occasionally in the white matter of the cord (data not shown) and in the cauda equina (Fig. 9) of all WNV-infected animals sectioned for these tissues.

NSE and TUNEL staining. To determine the involvement of apoptosis in neurons with persistent viral antigen, confocal microscopy was performed on spinal cord sections from WN02 (TX-114)-infected or from sham-infected hamsters at 40 dpi using specific antibodies for the WNV envelope, NSE, and TUNEL stain (Fig. 10). As observed previously (23), WNV staining was colocalized with NSE staining, which demonstrated the specific infection of neurons; however, some WNV

staining was not colocalized with NSE staining (Fig. 10A). TUNEL staining was apparent in the nuclei of some, but not all neurons; however, the TUNEL staining did not subjectively appear to be as intense as in the acute infection (24, 33) (Fig. 10C). Additionally, some TUNEL-stained cells were independent of the WNV staining. WNV and TUNEL staining of sham-injected animals was low and confirmed the specificity of the staining in infected animals (Fig. 10B and D).

DISCUSSION

To investigate the hypothesis that neurological sequelae are associated with persistent WNV and neuropathology, we developed an electrophysiological MUNE assay specific to hamsters to measure the health of motor neurons longitudinally in
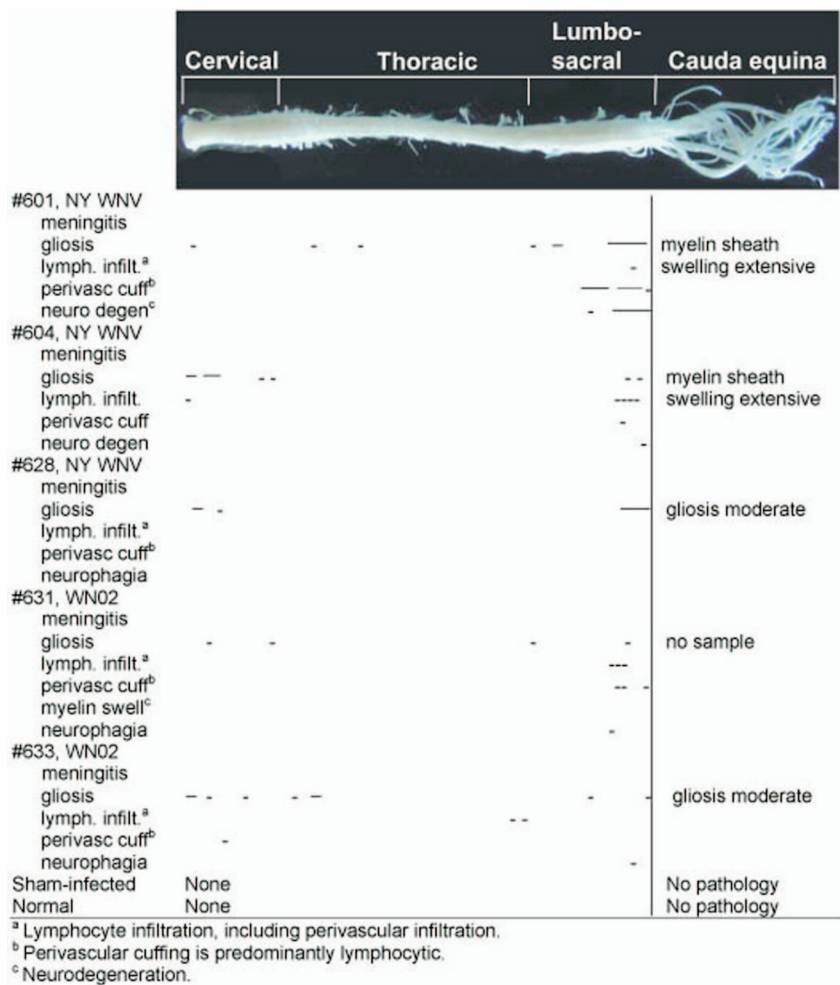
FIG. 9. Mapping neuropathology in the spinal cords of hamsters injected s.c. with WNV. Hamsters were injected s.c. with strain WN02 TX-113 or NY WNV (385-99). At 26 days after challenge, coronal pieces of the cervical cord were blocked in a cassette for sequential sectioning, as were the thoracic, lumbar/sacral, and cauda equina areas of the spinal cord. The first slide in each of five sections was processed for H&E staining. The cauda equina was cut longitudinally in the same manner as the coronal spinal cord sections (i.e., five sections, followed by a 50-μm gap), repeated until the tissue was completely sectioned. Lines were used to map the locations of the lesions within the spinal cord.

hamsters. MUNE was suppressed beginning 8 days after s.c. injection of the WN02 strain and remained suppressed out to 92 days. The utility of MUNE elucidated mechanisms of pathogenesis in this neurological sequela, namely, that WNV antigen or virus can persist in neurons to cause dysfunction, that WNV is associated with chronic neuropathological lesions, and that this neurological sequela is nearly a universal event in WNV-infected hamsters under the conditions investigated.

α-Motor neurons, large motor neurons in the anterior horn of the spinal cord (ventral horn in horizontal animals), are one of the primary targets in ALS (5), poliovirus (21), and for WNV (24). More specifically, WNV has been described as causing poliomyelitis-like disease, since it infects motor neurons in the anterior horn of the spinal cord (10, 24). Since MUNE provides a sensitive marker for the progression of ALS (5) and polio (3), we anticipated correctly that it would also be a sensitive marker for West Nile neuroinvasive disease in the spinal cord.

All of the hamsters infected s.c. with WNV were identified to have suppressed MUNE after day 10 of infection and some as early as 8 days. This uniform identification of neurological

spinal cord disease is remarkable considering the variable disease phenotypes that can be observed in these hamsters (23): i.e., some hamsters can have variable combinations of paralysis, eye lacrimation, or tremors, or some may die without any other disease signs besides mortality. Therefore, one might have expected some hamsters to have suppressed MUNE and others to be normal. Nevertheless, all hamsters in Fig. 1 infected with WN02 eventually had suppressed MUNE in the chronic infection. This uniformity of detection may be attributable to MUNE's sensitivity, since even asymptomatic animals showing no overt disease signs still had reduced MUNE when assayed after establishment of infection in the CNS (data not shown).

The identification of suppressed MUNE in the acute phase and long thereafter led us to investigate the neuropathology and persistent WNV in the brain and spinal cord. In the acute infection, hamsters at day 10 with diminished MUNE were extensively infected with WN02 in the brain and spinal cord and, more specifically, in the lumbosacral cord as evidenced by the presence of WNV RNA, infectious virus, and WNV immunohistochemistry (data not shown). Significant MUNE suppression was first ob-
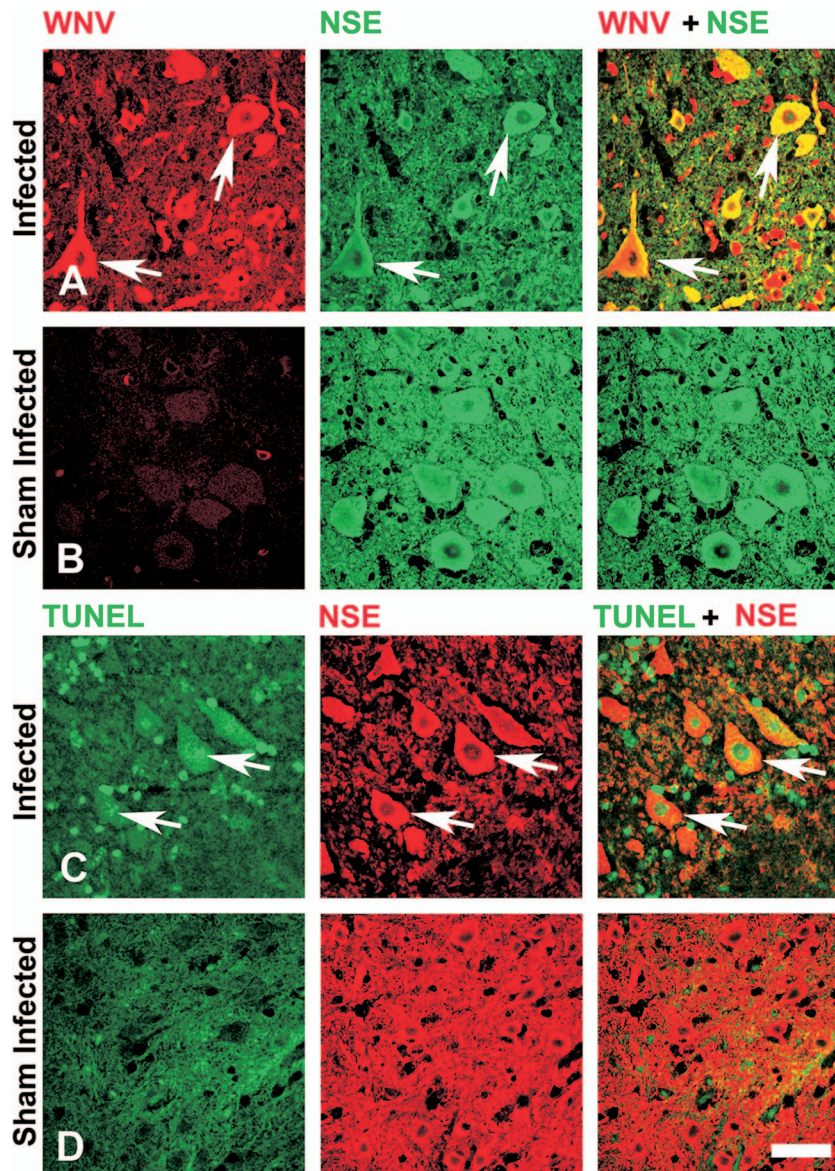
FIG. 10. Confocal images of the spinal cord sections double stained for viral and cellular markers. The coronal sections of the spinal cord gray matter were double stained for WNV envelope and NSE (A and B) and for TUNEL and NSE (C and D) in hamsters 40 days after s.c. injection with WNV (WN02 TX-114) (A and C) or sham infection (B and D). Arrows show the double-stained cell. Scale bar, 20 μm.

served 8 days after s.c. injection of WNV, yet neurons are infected in the CNS by day 5 (23). This delay in reduced MUNE might be explained by the damage of the neuron bodies, followed by a delay of axonal dysfunction. The temporal development of neuronal cell damage in the spinal cord in the acute infection followed by the chronic infection is reminiscent in some ways of ALS and poliomyelitis. The motor units consisting of cell bodies, axons, and the muscle fibers are diminished, probably due to cell body damage followed by axonal degeneration (30).

Suppression of MUNE was coincident with the presence of WNV-induced neuropathology, whereas MUNE was not suppressed in hamsters infected with yellow fever virus or Punta Toro virus, which cause nonneurological diseases. Moreover, MUNE correlated with disease phenotype, because the lowest MUNE values observed in these studies were detected in par-

alyzed limbs. Additionally, suppressed MUNE correlated ($R^2 = 0.91$) with suppressed ChAT staining of α-motor neurons of the ventral lumbosacral cord, but not with the number of α-motor neurons as determined by Nissl staining. The affected neurons lost function as determined by suppressed MUNE, but did not die in detectable numbers before day 10, which indicated that suppressed function can cause suppressed MUNE. Some motor neurons do eventually die between days 10 and 26. After day 26 to day 35, motor neurons did not continue to die since their numbers were not decreasing according to Nissl staining during this period. This suggests that dysfunctional motor neurons can eventually die during a window of time in the infection, but some infected neurons continue to survive into the chronic phase of the disease.

The observation of suppressed MUNE led to the detection

of persistent WNV in hamsters. Immunohistochemistry consistently revealed WNV envelope-positive cells throughout the CNS. WNV RNA was also detected in all neurological tissues of all nine WNV-infected hamsters assayed between 28 to 89 dpi, although the relative amount of RNA varied by nearly 4 logs. Infectious virus was only isolated from 3 of 54 tissues assayed. Prior animal studies suggest that neuropathology persists after viral load is reduced, but it was not known if neuropathology can persist with the complete absence of virus or if low-level persistent virus or its products are required for maintenance of neuropathology (13). In a 1983 study (27), WNV was isolated from rhesus monkey brains up to 5½ months after intracerebral inoculations, wherein, the phenotype of the isolated virus was altered. Over time, the phenotype of isolated viruses from the brain changed as evidenced by a loss of neurovirulence in mice and cytopathic properties in cell culture. The monkeys from which these viruses were isolated possessed subacute inflammatory neurodegeneration of the CNS.

As with these earlier primate studies, the virus in this report may have also undergone genotypic and phenotypic changes, because of the difficulty of recovering virus from only 3 of 54 tissues, where all 54 tissues were positive for WNV RNA by PCR. Genotypic changes might confer properties of persistent infection to the virus, possibly by evading the innate or adaptive immune responses. More recently, WNV was also isolated predominantly from the urine and kidneys but not the brains of hamsters inoculated intraperitoneally with WNV (42, 43). The persistent viruses isolated from the urine of these hamsters were determined to have lost neurovirulence with concomitant genotypic changes in the coding regions (45). As with the primate studies, the viruses isolated from the hamsters were genotypically and phenotypically altered (9). The genotypic and phenotypic changes of the recovered WNV herein await further investigation. In humans, the persistence of IgM in some infected people suggests long-term WNV-antigenic stimulation, possibly from persistent virus or protein (17).

An important question is if persistent virus or its proteins are biologically relevant. We addressed this by correlating WNV with the neuropathology. Adjacent serial tissue sections stained for WNV envelope antigen and by H&E allowed us to establish the correlation of neuropathology with WNV envelope: i.e., serial tissues with neuropathological lesions were associated with WNV staining, whereas, normal tissues were not associated with WNV staining. In tissues with meningitis, many lymphoid-like cells infiltrating meninges were positively stained for WNV envelope antigen. The identity of these positively stained cells is yet to be determined. Likewise, in tissues with perivascular cuffing or lymphocytic infiltration, lymphoid-like cells were also stained with WNV. These data suggest that immunoreactivity is involved in some of the WNV pathology during the chronic phase of the disease. In addition, WNV-stained motor neurons were present in the ventral horn of the spinal cord. Glial cells or astrocytes were not obviously stained for WNV antigen, although low levels of virus infection could be present if below the limits of detection; we have observed WNV infection of these cells in other experiments of other studies (data not shown). Dramatic evidence that persistent WNV was directly associated with neuropathology is the colocalization of WNV antigen staining with Wallerian degeneration or axonal swelling in selective axon bundles that are adjacent to uninfected axon bundles possessing no pathology at days 26 and 106. Because the antibody stained for the envelope protein, the axon bundles contained either viral particles or viral protein. Notably, the axon bundles were typically void of lymphocytic infiltration, which suggests that the virus or its proteins directly caused the axonal pathology. A correlation of the presence of viral proteins or particles with neuropathology does not necessarily mean that viral titers would strongly correlate with neuropathology or MUNE. We conducted an experiment that revealed that WNV RNA titers did not, in fact, correlate well with MUNE (data not shown). Therefore, the presence of the viral envelope, as detected by immunohistochemistry, was a correlate for disease, but the levels of viral RNA were not. The involvement of infectious virus or just viral products in persistent neurological lesions, therefore, awaits further investigation.

The striking contrast between uninfected and infected caudal axon bundles adjacent to one other is further evidence of retrograde or antegrade axonal transport of WNV (33). Since WNV appears to have a tropism for α-motor neurons in the ventral horn, one can speculate that the WNV-stained axon bundles originate from α-motor neurons. To our knowledge, this is the first example of homogeneous viral staining of an axon bundle, but not in adjacent bundles, that may reflect axonal transport originating from α-motor neurons preferentially infected by WNV. This may have clinical relevance because magnetic resonance imaging in human WNV-meningoencephalitis includes abnormal signal intensity more pronounced in the ventral horns and/or enhancement around the cauda equina (1, 26).

We have constructed the following model of WNV pathogenesis in the spinal cord of hamsters. Motor neurons in the ventral horn of the spinal cord are primarily infected either by hematogenous routes or by retrograde infection (33). By day 10 after s.c. viral challenge, MUNE suppression correlates exceptionally well with loss of ChAT staining measuring the function of motor neurons, but the numbers of α-motor neurons in the spinal cord are unaffected compared to those in sham-infected animals. By day 26, however, some motor neurons (18% to 28%) die, but they do not continue to die past day 26. During this later stage of infection, the motor neurons and their associated axons possessing either WNV or its proteins are dysfunctional, which causes suppressed MUNE and paralysis or muscle weakness. Since these neuronal cells survive, compensatory axonal sprouting from adjacent healthy axons (30) will not replace the dysfunctional axons, so both suppressed MUNE and muscle weakness may persist in some patients. The correlate to this hypothesis is that neurological sequelae might be reduced if the viral load is reduced by innate or acquired immunity or by antiviral therapy in the long-term phase of the disease.

In summary, this study establishes that WNV persists in neurons to cause dysfunction, that WNV envelope-stained cells are associated with chronic neuropathological lesions, and that this neurological sequela in the spinal cord as measured by MUNE is nearly a universal event in WNV-infected hamsters. MUNE may be a useful clinical marker in acutely infected patients and during neurological sequelae inasmuch as MUNE has been correlated with WNV-induced muscle weakness and lack of recovery in human patients (2) and WNV-infected humans can also experience a poliomyelitis-like disease (35) in which motor neurons are damaged.

REFERENCES

1. **Ali, M., Y. Safriel, J. Sohi, A. Llave, and S. Weathers.** 2005. West Nile virus infection: MR imaging findings in the nervous system. AJNR Am. J. Neuroradiol. **26:**289–297.
2. **Cao, N. J., C. Ranganathan, W. J. Kupsky, and J. Li.** 2005. Recovery and prognosticators of paralysis in West Nile virus infection. J. Neurol. Sci. **236:**73–80.
3. **Chan, K. M., N. Amirjani, M. Sumrain, A. Clarke, and F. J. Strohschein.** 2003. Randomized controlled trial of strength training in post-polio patients. Muscle Nerve **27:**332–338.
4. **Chu, J. J., and M. L. Ng.** 2003. The mechanism of cell death during West Nile virus infection is dependent on initial infectious dose. J. Gen. Virol. **84:**3305–3314.
5. **Dantes, M., and A. McComas.** 1991. The extent and time course of motoneuron involvement in amyotrophic lateral sclerosis. Muscle Nerve **14:**416–421.
6. **Darman, J., S. Backovic, S. Dike, N. J. Maragakis, C. Krishnan, J. D. Rothstein, D. N. Irani, and D. A. Kerr.** 2004. Viral-induced spinal motor neuron death is non-cell-autonomous and involves glutamate excitotoxicity. J. Neurosci. **24:**7566–7575.
7. **Davis, C. T., D. W. Beasley, H. Guzman, M. Siirin, R. E. Parsons, R. B. Tesh, and A. D. Barrett.** 2004. Emergence of attenuated West Nile virus variants in Texas, 2003. Virology **330:**342–350.
8. **Davis, J. W., and J. L. Hardy.** 1974. Characterization of persistent Modoc viral infections in Syrian hamsters. Infect. Immun. **10:**328–334.
9. **Ding, X., X. Wu, T. Duan, M. Siirin, H. Guzman, Z. Yang, R. B. Tesh, and S. Y. Xiao.** 2005. Nucleotide and amino acid changes in West Nile virus strains exhibiting renal tropism in hamsters. Am. J. Trop. Med. Hyg. **73:**803–807.
10. **Doron, S. I., J. F. Dashe, L. S. Adelman, W. F. Brown, B. G. Werner, and S. Hadley.** 2003. Histopathologically proven poliomyelitis with quadriplegia and loss of brainstem function due to West Nile virus infection. Clin. Infect. Dis. **37:**e74–e77.
11. **Garcia-Tapia, D., D. E. Hassett, W. J. Mitchell, Jr., G. C. Johnson, and S. B. Kleiboeker.** 2007. West Nile virus encephalitis: sequential histopathological and immunological events in a murine model of infection. J. Neurovirol. **13:**130–138.
12. **Gowen, B. B., J. W. Judge, M. H. Wong, K. H. Jung, C. F. Aylsworth, P. C. Melby, B. Rosenberg, and J. D. Morrey.** 2008. Immunoprophylaxis of Punta Toro virus (Phlebovirus, Bunyaviridae) infection in hamsters with recombinant Eimeria profilin-like antigen. Int. Immunopharmacol. **8:**1089–1094.
13. **Hayes, E. B., J. J. Sejvar, S. R. Zaki, R. S. Lanciotti, A. V. Bode, and G. L. Campbell.** 2005. Virology, pathology, and clinical manifestations of West Nile virus disease. Emerg. Infect. Dis. **11:**1174–1179.
14. **Julander, J. G., J. D. Morrey, L. M. Blatt, K. Shafer, and R. W. Sidwell.** 2006. Comparison of the inhibitory effects of interferon alfacon-1 and ribavirin on yellow fever virus infection in a hamster model. Antivir. Res. **73:**140–146.
15. **Julander, J. G., Q. A. Winger, A. L. Olsen, C. W. Day, R. W. Sidwell, and J. D. Morrey.** 2005. Treatment of West Nile virus-infected mice with reactive immunoglobulin reduces fetal titers and increases dam survival. Antivir. Res. **65:**79–85.
16. **Julander, J. G., Q. A. Winger, L. F. Rickords, P. Y. Shi, M. Tilgner, H. M. Gavin, R. W. Sidwell, and J. D. Morrey.** 2006. West Nile virus infection of the placenta. Virology **347:**175–182.
17. **Kapoor, H., K. Signs, P. Somsel, F. P. Downes, P. A. Clark, and J. P. Massey.** 2004. Persistence of West Nile Virus (WNV) IgM antibodies in cerebrospinal fluid from patients with CNS disease. J. Clin. Virol. **31:**289–291.
18. **Lanciotti, R. S., G. D. Ebel, V. Deubel, A. J. Kerst, S. Murri, R. Meyer, M. Bowen, N. McKinney, W. E. Morrill, M. B. Crabtree, L. D. Kramer, and J. T. Roehrig.** 2002. Complete genome sequences and phylogenetic analysis of West Nile virus strains isolated from the United States, Europe, and the Middle East. Virology **298:**96–105.
19. **Lanciotti, R. S., and A. J. Kerst.** 2001. Nucleic acid sequence-based amplification assays for rapid detection of West Nile and St. Louis encephalitis viruses. J. Clin. Microbiol. **39:**4506–4513.
20. **Mathur, A., K. L. Arora, S. Rawat, and U. C. Chaturvedi.** 1986. Persistence, latency and reactivation of Japanese encephalitis virus infection in mice. J. Gen. Virol. **67:**381–385.
21. **McComas, A. J., C. Quartly, and R. C. Griggs.** 1997. Early and late losses of motor units after poliomyelitis. Brain **120:**1415–1421.
22. **Morrey, J. D., V. Siddharthan, A. L. Olsen, G. Y. Roper, H. C. Wang, T. J. Baldwin, S. Koenig, S. Johnson, J. L. Nordstrom, and M. S. Diamond.** 2006.

23. Humanized monoclonal antibody against West Nile virus E protein administered after neuronal infection protects against lethal encephalitis in hamsters. J. Infect. Dis. **194:**1300–1308.
23. **Morrey, J. D., V. Siddharthan, A. L. Olsen, H. Wang, J. G. Julander, J. O. Hall, H. Li, J. L. Nordstrom, S. Koenig, S. Johnson, and M. S. Diamond.** 2007. Defining limits of treatment with humanized neutralizing monoclonal antibody for West Nile virus neurological infection in a hamster model. Antimicrob. Agents Chemother. **51:**2396–2402.
24. **Morrey, J. D., V. Siddharthan, H. Wang, J. O. Hall, R. T. Skirpstunas, J. L. Nordstrom, S. Koenig, S. Johnson, and M. S. Diamond.** 2008. West Nile virus-induced acute flaccid paralysis is prevented by monoclonal antibody treatment even after infection of spinal cord neurons. J. Neurovirol. **14:**152–163.
25. **Ohka, S., and A. Nomoto.** 2001. Recent insights into poliovirus pathogenesis. Trends Microbiol. **9:**501–506.
26. **Petropoulou, K. A., S. M. Gordon, R. A. Prayson, and P. M. Ruggierri.** 2005. West Nile virus meningoencephalitis: MR imaging findings. AJNR Am. J. Neuroradiol. **26:**1986–1995.
27. **Pogodina, V. V., M. P. Frolova, G. V. Malenko, G. I. Fokina, G. V. Koreshkova, L. L. Kiseleva, N. G. Bochkova, and N. M. Ralph.** 1983. Study on West Nile virus persistence in monkeys. Arch. Virol. **75:**71–86.
28. **Pogodina, V. V., L. S. Levina, G. I. Fokina, G. V. Koreshkova, G. V. Malenko, N. G. Bochkova, and O. E. Rzhakhova.** 1981. Persistence of tick-borne encephalitis virus in monkeys. III. Phenotypes of the persisting virus. Acta Virol. **25:**352–360.
29. **Pogodina, V. V., G. V. Malenko, G. I. Fokina, L. S. Levina, G. V. Koreshkova, O. E. Rzhakhova, N. G. Bochkova, and L. L. Mamonenko.** 1981. Persistence of tick-borne encephalitis virus in monkeys. II. Effectiveness of methods used for virus detection. Acta Virol. **25:**344–351.
30. **Rashidipour, O., and K. M. Chan.** 2008. Motor unit number estimation in neuromuscular disease. Can. J. Neurol. Sci. **35:**153–159.
31. **Samuel, M. A., and M. S. Diamond.** 2005. Alpha/beta interferon protects against lethal West Nile virus infection by restricting cellular tropism and enhancing neuronal survival. J. Virol. **79:**13350–13361.
32. **Samuel, M. A., J. D. Morrey, and M. S. Diamond.** 2006. Caspase 3-dependent cell death of neurons contributes to the pathogenesis of West Nile virus encephalitis. J. Virol. **81:**2614–2623.
33. **Samuel, M. A., H. Wang, V. Siddharthan, J. D. Morrey, and M. S. Diamond.** 2007. Axonal transport mediates West Nile virus entry into the central nervous system and induces acute flaccid paralysis. Proc. Natl. Acad. Sci. USA **104:**17140–17145.
34. **Sejvar, J. J.** 2007. The long-term outcomes of human West Nile virus infection. Clin. Infect. Dis. **44:**1617–1624.
35. **Sejvar, J. J., A. A. Leis, D. S. Stokic, J. A. Van Gerpen, A. A. Marfin, R. Webb, M. B. Haddad, B. C. Tierney, S. A. Slavinski, J. L. Polk, V. Dostrow, M. Winkelmann, and L. R. Petersen.** 2003. Acute flaccid paralysis and West Nile virus infection. Emerg. Infect. Dis. **9:**788–793.
36. **Shefner, J. M., M. Cudkowicz, and R. H. Brown, Jr.** 2006. Motor unit number estimation predicts disease onset and survival in a transgenic mouse model of amyotrophic lateral sclerosis. Muscle Nerve **34:**603–607.
37. **Shefner, J. M., M. E. Cudkowicz, and R. H. Brown, Jr.** 2002. Comparison of incremental with multipoint MUNE methods in transgenic ALS mice. Muscle Nerve **25:**39–42.
38. **Shrestha, B., D. Gottlieb, and M. S. Diamond.** 2003. Infection and injury of neurons by West Nile encephalitis virus. J. Virol. **77:**13203–13213.
39. **Shrestha, B., T. Wang, M. A. Samuel, K. Whitby, J. Craft, E. Fikrig, and M. S. Diamond.** 2006. Gamma interferon plays a crucial early antiviral role in protection against West Nile virus infection. J. Virol. **80:**5338–5348.
40. **Siirin, M. T., T. Duan, H. Lei, H. Guzman, A. P. da Rosa, D. M. Watts, S. Y. Xiao, and R. B. Tesh.** 2007. Chronic St. Louis encephalitis virus infection in the golden hamster (Mesocricetus auratus). Am. J. Trop. Med. Hyg. **76:**299–306.
41. **Sitati, E. M., and M. S. Diamond.** 2006. CD4⁺ T-cell responses are required for clearance of West Nile virus from the central nervous system. J. Virol. **80:**12060–12069.
42. **Tesh, R. B., M. Siirin, H. Guzman, A. P. Travassos da Rosa, X. Wu, T. Duan, H. Lei, M. R. Nunes, and S. Y. Xiao.** 2005. Persistent West Nile virus infection in the golden hamster: studies on its mechanism and possible implications for other flavivirus infections. J. Infect. Dis. **192:**287–295.
43. **Tonry, J. H., S. Y. Xiao, M. Siirin, H. Chen, A. P. da Rosa, and R. B. Tesh.** 2005. Persistent shedding of West Nile virus in urine of experimentally infected hamsters. Am. J. Trop. Med. Hyg. **72:**320–324.
44. **Weber, U. J., T. Bock, K. Buschard, and B. Pakkenberg.** 1997. Total number and size distribution of motor neurons in the spinal cord of normal and EMC-virus infected mice—a stereological study. J. Anat. **191:**347–353.
45. **Wu, X., L. Lu, H. Guzman, R. B. Tesh, and S. Y. Xiao.** 2008. Persistent infection and associated nucleotide changes of West Nile virus serially passaged in hamsters. J. Gen. Virol. **89:**3073–3079.
46. **Xiao, S. Y., H. Guzman, H. Zhang, A. P. Travassos da Rosa, and R. B. Tesh.** 2001. West Nile virus infection in the golden hamster (Mesocricetus auratus): a model for West Nile encephalitis. Emerg. Infect. Dis. **7:**714–721.